Numerical Simulation of Static Cracks using Extended Isogeometric Analysis

G. Bhardwaj
Department of Mechanical and Industrial Engineering
Indian Institute of Technology Roorkee,
Roorkee, India
er.gaganbhardwaj@gmail.com

I. V. Singh
Department of Mechanical and Industrial Engineering
Indian Institute of Technology Roorkee,
Roorkee, India
ivsingh@gmail.com

***Abstract*— In last decade, isogeometric analysis (IGA) has gained a lot of interest among the scientific community in solving various engineering problems. Nowadays, IGA has been extended to many scientific and engineering areas including fracture mechanics. This paper presents the simulation of stationary plane crack problems using extended isogeometric analysis (XIGA). In XIGA, both geometry and solution are approximated using NURBS basis functions. Heaviside function is used to model the crack face, while crack tip singularity is modeled using asymptotic crack tip enrichment functions. The various crack problems i.e. left edge crack, centre crack and double edge crack are solved using XIGA. The value of stress intensity factor (SIFs) is computed using domain based interaction integral approach. These simulations showed that SIF obtained using XIGA with higher order NURBS basis functions provide more accurate results as compared to those obtained by XFEM.**

Keywords—Edge crack; NURBS; Extended Isogeometric analysis (XIGA); Discontinuities; Enrichment Functions;

I. INTRODUCTION

Nowadays, most of the engineering problems are solved using FEM. It suffers from the disadvantage of conformal meshing for solving fracture problems. In present, the fracture analysis of structures is presented by the combination of isogeometric analysis (IGA) and XFEM. In IGA [1], the same (non-uniform rational B-splines i.e. NURBS) basis functions are used for defining the geometry as well for analysis. So far, the IGA have been successfully implemented in various fields such as gradient damage modeling [2], cohesive zone modeling [3] and topology optimization [4]. The implementation of NURBS based IGA for contact problems [5] gives greater accuracy and faster convergence rate as compared to the Lagrange based finite elements. Nearly same accuracy is achieved using NURBS based IGA with fewer degrees of freedom in fracture mechanics problems [6-7]. The different problems of stationary as well as propagating crack [8] are solved using extended isogeometric analysis (XIGA). The bi-material body with a curved interface [9] is analyzed by combination of quadratic NURBS basis function and XFEM. Free vibration analysis of thin plates done using a NURBS-based isogeometric approach [16]. The governing and discretized equation for free vibration analysis of Kirchhoff thin plates is obtained using standard Galerkin method. First-order, shear-deformable laminate composite plate theory is utilized in deriving the governing equations using a variational formulation for the non-linear analysis of laminated composite plates [17].

In the present work, XIGA is used for the simulation of planar crack problems. Edge crack, center crack and double edge crack problems are solved using XIGA. The effect of crack length and crack inclination is seen on the stress intensity factor. The value of stress intensity factor (SIFs) is computed using domain based interaction integral approach. It is concluded that the value of SIF increases with increase in the crack length and the value of SIF decreases with increase in crack inclination.

II. ISOGEOMETRIC ANALYSIS

A. Basis Function

The knot vector, B-spline and NURBS basis function are discussed in this section. B-splines basis functions are built from piecewise polynomial functions. The details of NURBS can be seen in [10]. The knot vector Ξ is defined by a set of coordinates, or knots, which gives information where the subintervals are connected. $\Xi = \{\xi_1, \xi_2, ...\xi_{n+p+1}\}$ are the real coordinates represent the geometry in parametric space [0, 1], where ξ_i is the i^{th} knot, i is the knot index, i = 1, 2... $n+p+1$, p and n are the polynomial order and number of basis function respectively used to construct the B-spline curve.

In the isogeometric analysis, different types of knot vectors are used i.e. open knot vector and closed knot vector. In the present analysis, open knot vector is used where end knots are repeated $p+1$ times. B-spline basis are defined recursively starting with $p=0$ in the following manner [10].

$$N_{i,0} = \begin{cases} 1 & \xi_i \le \xi \le \xi_{i+1} \\ 0 & otherwise \end{cases} \tag{1}$$

$$N_{i,p}(\xi) = \frac{\xi - \xi_i}{\xi_{i+p} - \xi_i} N_{i,p-1}(\xi) + \frac{\xi_{i+p+1} - \xi}{\xi_{i+p+1} - \xi_{i+1}} N_{i+1,p-1}(\xi) \tag{2}$$

The derivatives of B-spline basis function can be calculated for a given order of polynomial and knot vector.

$$\frac{dN_{i,p}(\xi)}{d\xi} = \frac{p}{\xi_{i+p}-\xi_i} N_{i,p-1}(\xi) - \frac{p}{\xi_{i+p+1}-\xi_{i+1}} N_{i+1,p-1}(\xi) \quad (3)$$

A rational B-spline curve defined by $n+1$ control points B_i is given by [10].

$$P(x) = \sum_{i=0}^{n} B_i R_{i,p}(x) \quad (4)$$

Rational B-spline basis functions $R_{i,k}(\xi)$ are defined in the following manner.

$$R_{i,p}(\xi) = \frac{w_i N_{i,p}(\xi)}{W(\xi)} = \frac{w_i N_{i,p}(\xi)}{\sum_{i=0}^{n} w_i N_{i,p}(\xi)} \quad (5)$$

where, $R_{i,p}(\xi)$ are the NURBS basis function, B_i defines coordinates of control point (X_i, Y_i), w_i represents the weights associated with control points and $N_{i,p}(\xi)$ defines the *B*-spline basis function of order *p* defined using knot vector. The length of the knot vector is given as [11].

$$m = n + p + 1 \quad (6)$$

The derivative of NURBS basis function can be computed as

$$\frac{dR_{i,p}(\xi)}{d\xi} = w_i \frac{W(\xi)N'_{i,p}(\xi) - W'(\xi)N_{i,p}(\xi)}{(W(\xi))^2} \quad (7)$$

NURBS has the following features

- NURBS basis function forms a partition of unity $\sum_{i=1}^{n} R_{i,p}(\xi) = 1$.
- The support of each $R_{i,p}(\xi)$ is compact and contained in interval [ξ_i, ξ_{i+p+1}].
- NURBS ensure $p-1$ continuous derivatives if internal knots are not repeated, whereas it produces C^{p-k} continuity if knot has multiplicity k.

B. Isogeometric Discretization

A given domain is partitioned into displacement Γ_u, traction Γ_t and traction free boundaries Γ_c. The equilibrium equation and boundary conditions are defined as [12]

$$\nabla.\sigma + b = 0 \text{ in } \Omega \quad (8)$$

$$\sigma.\hat{n} = \bar{t} \quad on \ \Gamma_t \quad (9)$$

$$\sigma.\bar{n} = 0 \quad \text{on } \Gamma_c \quad (10)$$

where, $\boldsymbol{\sigma}$ is Cauchy stress tensor and $\mathbf{b}$ is body force per unit volume.

The constitutive relation for the elastic material under consideration is given by Hook's law:

$$\boldsymbol{\sigma} = D\varepsilon \quad (11)$$

A weak form of the equilibrium equation [13] is given as:

$$\int_\Omega \boldsymbol{\sigma}(\mathbf{u}) : \varepsilon(\mathbf{v}) d\Omega = \int_\Omega \mathbf{b}.\mathbf{v} d\Omega + \int_{\Gamma_t} \bar{\mathbf{t}}.\mathbf{v} d\Gamma \quad (12)$$

On substituting the trial and test functions and using the arbitrariness of nodal variations, the following discrete system of equations are obtained

$$[\mathbf{K}]\{\mathbf{d}\} = \{\mathbf{f}\} \quad (13)$$

where, $\mathbf{K}$ is the global stiffness matrix, $\mathbf{d}$ is the vector of nodal unknowns and $\mathbf{f}$ is the external force vector. B matrix of basis function derivatives is given by [8]:

$$B = \begin{bmatrix} \frac{\partial R_1}{\partial X_1} & 0 & ..... & \frac{\partial Rn_{en}}{\partial X_1} & 0 \\ 0 & \frac{\partial R_1}{\partial X_2} & ..... & 0 & \frac{\partial Rn_{en}}{\partial X_2} \\ \frac{\partial R_1}{\partial X_2} & \frac{\partial R_1}{\partial X_1} & ..... & \frac{\partial Rn_{en}}{\partial X_2} & \frac{\partial Rn_{en}}{\partial X_1} \end{bmatrix} \quad (14)$$

where, $R(\xi)$ is a vector of NURBS basis functions, R_i ($i = 1, 2, ...n_{en}$) in parametric space of $\xi = (\xi_1, \xi_2)$. $n_{en} = (p+1)\times(q+1)$ represents the number of non-zero basis function for a given knot span i.e. element. The order of curve in ξ_1 and ξ_2 directions are defined by p and q respectively. The physical coordinates $X = (X_1, X_2)$ and displacement approximation u^h can be derived for a particular point $\xi = (\xi_1, \xi_2)$ i.e. parametric coordinate.

$$u^h(\xi) = \sum_{i=1}^{n_{en}} R_i(\xi) u_i \quad (15)$$

$$X(\xi) = \sum_{i=1}^{n_{en}} R_i(\xi) B_i \quad (16)$$

III. EXTENDED ISOGEOMETRIC ANALYSIS

In extended isogeometric analysis, the displacement approximation is locally enriched to simulate discontinuities. Few degrees of freedom are added to the selected control points near the location of a crack.

A. XIGA approximations for cracks

In XIGA, for modeling crack edge and tip, (15) can be written in generalized form as

$$u^h(\xi) = \sum_{i=1}^{n_{en}} R_i(\xi) u_i + \sum_{j=1}^{n_{cf}} R_j(\xi) H(\xi) a_j + \sum_{k=1}^{n_{ct}} R_k(\xi) (\sum_{\alpha=1}^{4} \beta_\alpha(\xi) b_k^\alpha) \quad (17)$$

where $H(\xi)$ and β_α are the Heaviside function and crack tip enrichment functions respectively. The additional degrees of freedom related to the modeling of crack face and crack tip are represented by vectors a_j and b_k^α respectively. The n_{cf} is the number of n_{en} basis function that have crack face in their support domain and n_{ct} is the number of basis function associated with crack tip in the domain of influence. Heaviside function $H(\xi)$ is +1 (if physical coordinates corresponding to parametric coordinates ξ) is above crack and -1 on the other side of discontinuity. The crack tip enrichment functions are defined as [12]:

$$\beta_\alpha(\xi) = [\sqrt{r}\cos\frac{\theta}{2}, \sqrt{r}\sin\frac{\theta}{2}, \sqrt{r}\cos\frac{\theta}{2}\cos\theta, \sqrt{r}\sin\frac{\theta}{2}\cos\theta]$$

where, r and θ are the local crack tip parameters.

B. XIGA formulation for a crack

The first term in the right hand side of (17) evaluates the displacement field by using classical IGA approximation, while remaining terms are enrichment approximation to model discontinuity and represents solution accurately near the crack tip. The elemental matrices $\mathbf{K}$ and $\mathbf{f}$ in (13), are obtained using the approximation function defined in (15).

$$\mathbf{K}_{ij}^{e} = \begin{bmatrix} K_{ij}^{uu} & K_{ij}^{ua} & K_{ij}^{ub} \\ K_{ij}^{au} & K_{ij}^{aa} & K_{ij}^{ab} \\ K_{ij}^{bu} & K_{ij}^{ba} & K_{ij}^{bb} \end{bmatrix} \quad (i, j = 1, 2, 3......n_{en}) \tag{18}$$

The discretized form of governing equation:

$$\mathbf{f}^{h} = \left\{ \mathbf{f}_i^{u} \quad \mathbf{f}_i^{a} \quad \mathbf{f}_i^{b1} \quad \mathbf{f}_i^{b2} \quad \mathbf{f}_i^{b3} \quad \mathbf{f}_i^{b4} \right\}^{T} \tag{19}$$

$$\mathbf{K}_{ij}^{rs} = \int_{\Omega^e} (\mathrm{B}_i^{r})^{T} \mathbf{C}\, \mathrm{B}_j^{s}\, h d\Omega \quad \text{where} \quad r, s = u, a, b, c, d \tag{20}$$

$$\mathbf{f}_i^{u} = \int_{\Omega^e} R_i^{T} \mathbf{b}\, d\Omega + \int_{\Gamma_t} R_i^{T} \bar{\mathbf{t}}\, d\Gamma \tag{21}$$

$$\mathbf{f}_i^{a} = \int_{\Omega^e} R_i^{T} H \mathbf{b}\, d\Omega + \int_{\Gamma_t} R_i^{T} H\, \bar{\mathbf{t}}\, d\Gamma \tag{22}$$

$$\mathbf{f}_i^{b\alpha} = \int_{\Omega^e} R_i^{T} \beta_\alpha \mathbf{b}\, d\Omega + \int_{\Gamma_t} R_i^{T} \beta_\alpha\, \bar{\mathbf{t}}\, d\Gamma \quad \text{Where,} \ \alpha = 1, 2, 3, 4 \tag{23}$$

where, R_i^{T} are represents the NURBS basis function. B_i^{u}, B_i^{a}, B_i^{b}, $\mathrm{B}_i^{b\alpha}$, B_i^{c} and B_i^{d} are the NURBS basis function derivatives matrices given by:

$$\mathrm{B}_i^{u} = \begin{bmatrix} R_{i,X_1} & 0 \\ 0 & R_{i,X_2} \\ R_{i,X_2} & R_{i,X_1} \end{bmatrix}_{3\times n_{en}}, \quad \mathrm{B}_i^{a} = \begin{bmatrix} (R_i)_{,X_1} H & 0 \\ 0 & (R_i)_{,X_2} H \\ (R_i)_{,X_2} H & (R_i)_{,X_1} H \end{bmatrix}_{3\times n_{en}}$$

$$\mathrm{B}_i^{b} = \begin{bmatrix} \mathrm{B}_i^{b1} & \mathrm{B}_i^{b2} & \mathrm{B}_i^{b3} & \mathrm{B}_i^{b4} \end{bmatrix} \quad \text{and}$$

$$\mathrm{B}_i^{b\alpha} = \begin{bmatrix} (R_i\beta_\alpha)_{,X_1} & 0 \\ 0 & (R_i\beta_\alpha)_{,X_2} \\ (R_i\beta_\alpha)_{,X_2} & (R_i\beta_\alpha)_{,X_1} \end{bmatrix}_{3\times n_{en}} \quad \text{where,} \ \alpha = 1, 2, 3, 4$$

C. Computation of Stress Intensity Factor

In the present work, the individual stress intensity factors K_I and K_{II} are obtained using domain form of interaction integral [15].

IV. NUMERICAL SIMULATION AND DISCUSSION

In the present work, edge crack problems are simulated using XIGA in the presence of inclusions and holes. In order to check the accuracy and performance of XIGA, the results are compared with XFEM. The order of NURBS basis function is taken 3 in both parametric directions, and weight of each control point taken as unity. First order NURBS with uniform weight is equivalent to the Lagrange finite elements. Uniformly distributed control points are taken for the analysis. The values of SIFs are computed using domain based interaction integral approach. The material properties [15] used for the simulations are:

Elastic Modulus $E = 74\,GPa$

Poisson Ratio for Material $\nu = 0.3$

Fracture Toughness $K_{IC} = 1897.36\ N/mm^{3/2}$

In the present work, edge crack, centre crack and double edge crack problems are simulated using XIGA. In order to check the accuracy and performance of XIGA, the results are compared with XFEM. The control points are taken to be 30×60 for the purpose of simulation. The knot vectors are taken open and uniform without any repetition. The bottom edge of the plate is constrained in the y direction. The plate is subjected to tensile load of $\sigma = 60\ N/mm$ at the top edge.

A. Plate with an edge crack and inclined crack

A plate of size $100\,\text{mm} \times 200\,\text{mm}$ along with a crack length $a = 30\,\text{mm}$ and with boundary conditions is shown in Fig. 1. The stress contour plot of σ_{yy} is depicted in Fig. 2. The theoretical stress intensity factor can be computed for left edge crack problem.

$$K_I = C\sigma\sqrt{\pi a} \tag{24}$$

$$C = \left[1.12 - 0.23\left(\frac{a}{L}\right) + 10.6\left(\frac{a}{L}\right)^2 - 21.7\left(\frac{a}{L}\right)^3 + 30.4\left(\frac{a}{L}\right)^4\right] \tag{25}$$

The stress intensity factor (SIF) varied with crack length and compared with exact results shown in Fig. 3. It has been observed that the value of SIF increases with increase in crack length. In second case, crack length kept constant ($a = 30$ mm) and crack angle is varied from 20 to 50 degree, then effect of crack angle is seen on the SIF. The results computed by using XIGA are compared with XFEM for crack angle variation shown in Fig. 4. It is evaluated that as crack angle increases, value of SIF decreases.

Table 1 presents the error in the mode-I SIF with the exact solution for different sets of control points, and NURBS order. From Table 1, it is predicted that as the NURBS order or the control points increases, the error in SIF starts decreasing.

Table 1: Error in mode-I SIF computed using XIGA and XFEM for a left edge crack

	Control Net/ Mesh			
	9 x18	12 x 24	22 x 42	42 x 82
	% error	% error	% error	% error
	XIGA	XIGA	XIGA	XIGA
1	3.46	2.64	1.66	0.0915
2	3.44	2.32	1.18	0.0611
3	3.20	1.15	1.04	0.0576

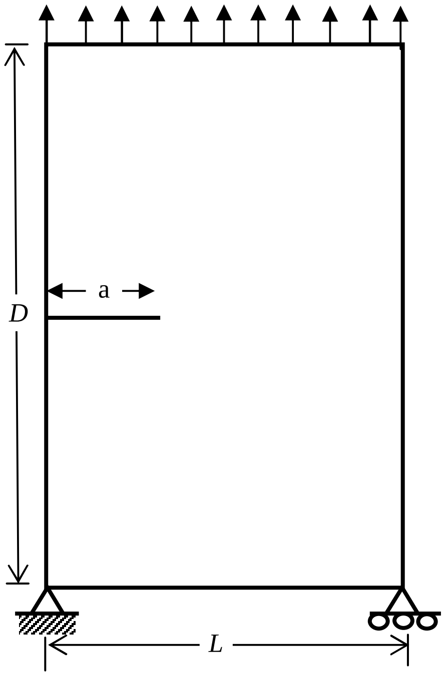

Fig. 1 Edge crack plate along with direction

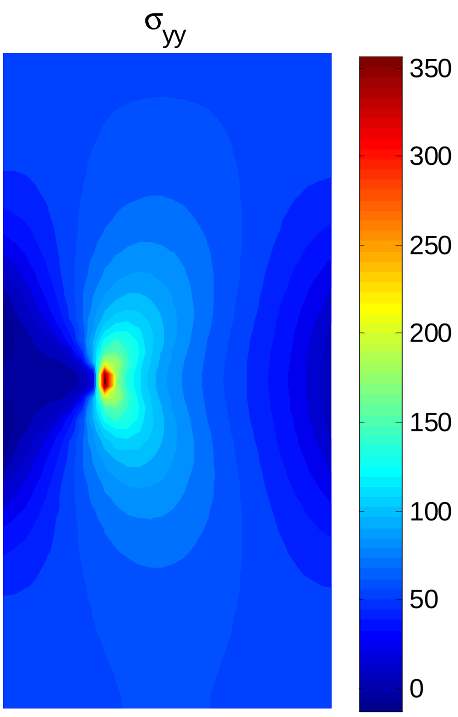

Fig. 2 Stress contour plot (σ_{yy}) for an edge crack plate

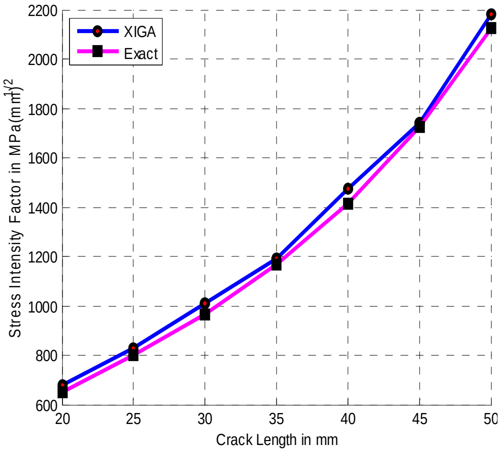

Fig. 3 SIF variation with crack length for a left edge crack problem

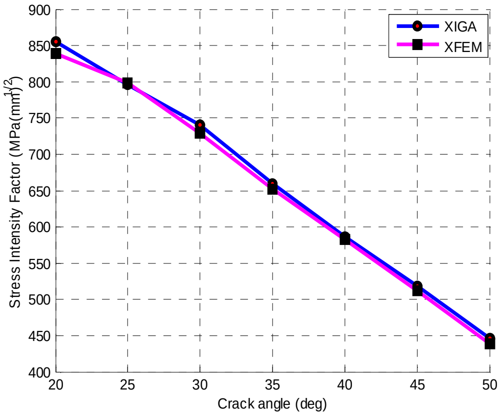

Fig. 4 SIF variation with crack angle for a left edge crack problem

B. Plate with centre crack and inclined centre crack

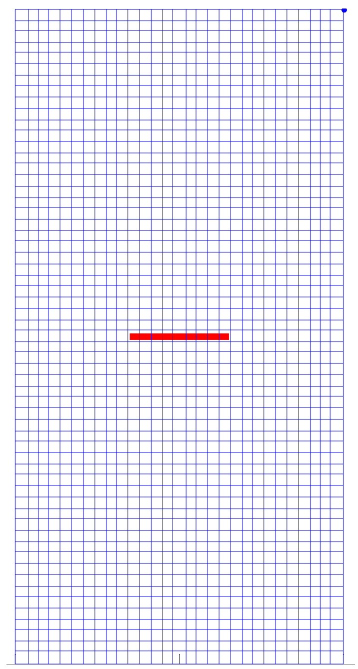

Fig. 5 Geometry of centre crack in plate

A plate of size $100\,\text{mm} \times 200\,\text{mm}$ along with a centre crack length $a = 30\,\text{mm}$ is shown in Fig. 5. The σ_{yy} represents the stress contour plot shown in Fig. 6. The SIF variation plotted with crack length and results are compared with exact solution shown in Fig. 7. In second case, crack length of centre crack is kept constant i.e. $a = 30\,\text{mm}$ and crack angle varied from 20 to 50 degree. The plot of SIFs with crack angle is depicted in Fig. 8 and the XIGA results are compared with the XFEM results. It has been concluded from plots that value of SIF increases with increase in crack length and value of SIF decreases with increase in crack angle.

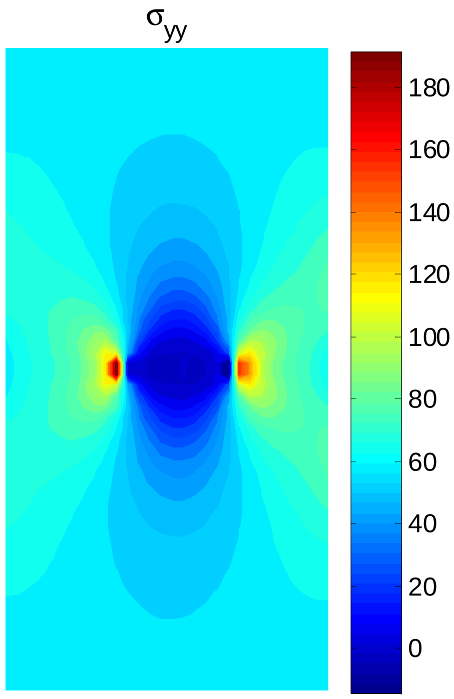

Fig. 6 Stress contour plot (σ_{yy}) for centre crack in plate

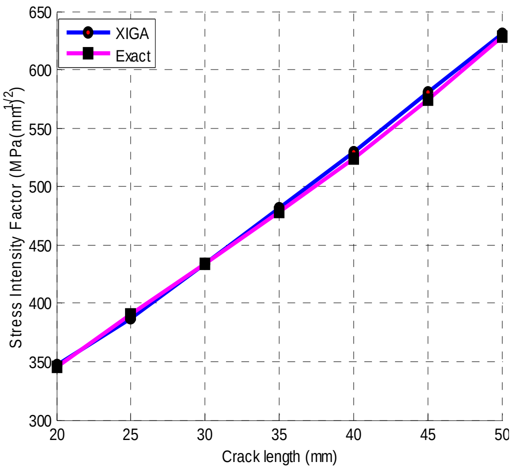

Fig. 7 SIF variation with crack length for centre crack

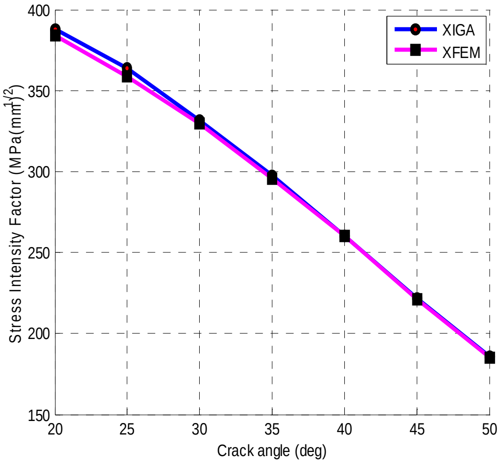

Fig. 8 SIF variation with crack angle for centre crack

C. Plate with double edge crack

In case of double edge crack, a plate of size $100\,\text{mm} \times 200\,\text{mm}$ along with crack length $a = 20\,\text{mm}$ is shown in Fig. 9. The contour plots of σ_{yy} is depicted in Fig. 10. In double edge crack problem, crack length of left crack is kept constant and length of right edge crack varied from 20 to 50 mm. The variation of SIF is plotted with crack length and shown in the Fig. 11. Now, the crack length of both edge cracks is kept constant and the angle of right edge crack is varied from 20 to 45 degree. The plot of SIF with crack angle is depicted in Fig. 12. It is concluded from plots that the value of SIF increases with increase in crack length and value of SIF decrease with increase in crack angle.

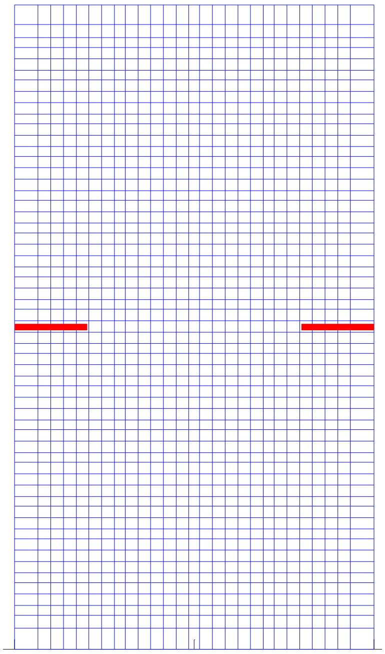

Fig. 9 Geometry of double edge crack in plate

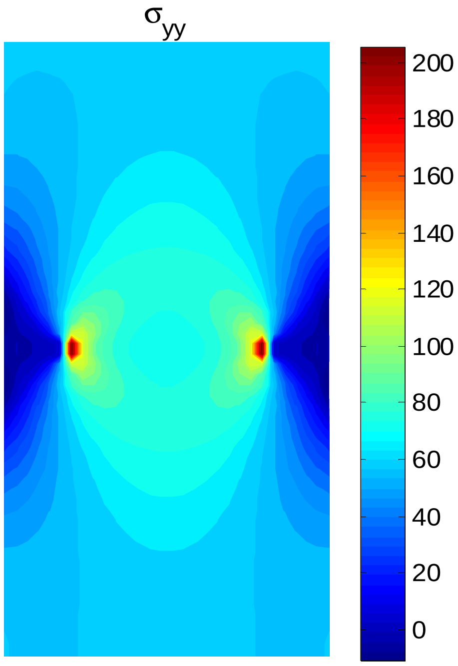

Fig. 10 Stress contour plot (σ_{yy}) for double edge crack in plate

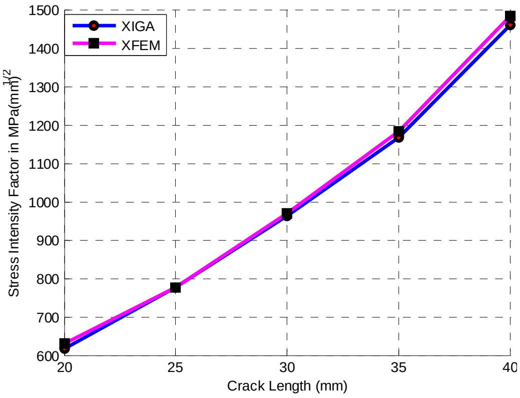

Fig. 11 SIF variation with crack length for double edge crack

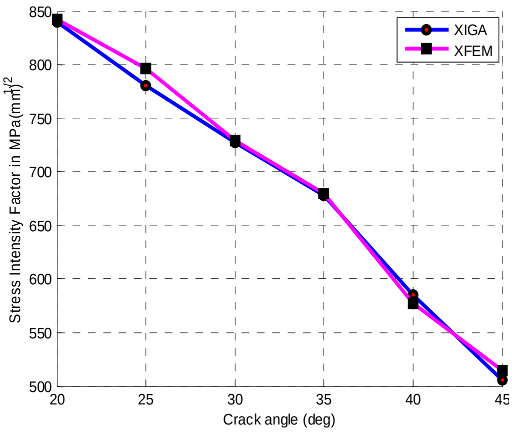

Fig. 12 SIF variation with crack angle for double edge crack

V. Conclusions

In the present work, XIGA has been used for the simulation of plane crack problems i.e. left edge crack, centre edge crack and double edge crack problems. Both the geometry and solution are defined using NURBS basis function. The SIF value is computed using domain based interaction integral approach. The SIF values are computed using XIGA gives good agreement with exact solution in case of left edge crack and centre crack problem. The SIF values are evaluated with variation in crack angle and then compared with XFEM results. These simulations show that the greater accuracy achieved using higher order NURBS basis function as compared to XFEM. It is concluded that the value of SIF increases with increase in the crack length and the value of SIF decreases with increase in crack inclination.

References

[1] T.J.R. Hughes, J.A. Cottrell, and Y. Bazilevs, "Isogeometric analysis: CAD, finite elements, NURBS, exact geometry and mesh refinement," Computer Methods in Applied Mechanics and Engineering, vol. 194, pp. 4135-4195, 2005.

[2] C.V. Verhoosel, M.A. Scott, T.J.R. Hughes, and R.D Borst, "An isogeometric analysis approach to gradient damage models," International Journal for Numerical Methods in Engineering, vol. 86, pp. 115-134, 2011.

[3] C.V. Verhoosel, M.A. Scott, R.D. Borst, and T.J.R. Hughes, "An isogeometric approach to cohesive zone modeling," International Journal for Numerical Methods in Engineering, vol. 87, pp. 336-360, 2011.

[4] B. Hassani, M. Khanzadi, and S.M. Tavakkoli, "An isogeometrical approach to structural topology optimization by optimality criteria," Structural and multidisciplinary optimization, vol. 45, pp. 223-233, 2012.

[5] I. Temizer, P. Wriggers, and T.J.R. Hughes, "Contact treatment in isogeometric analysis with NURBS," Computer Methods in Applied Mechanics and Engineering, vol. 200, pp. 1100-1112, 2011.

[6] E. De Luycker, D.J. Benson, T. Belytschko, Y. Bazilevs, and M. C. Hsu, "X-FEM in isogeometric analysis for linear fracture mechanics," International Journal for Numerical Methods in Engineering, vol. 87, pp. 541-565, 2011.

[7] D.J. Benson, Y. Bazilevs, E. De. Luycker, M.C. Hsu, M.A Scott, T.J.R. Hughes, and T. Belytschko, "A generalized finite element formulation for arbitrary basis functions: From isogeometric analysis to XFEM," International Journal for Numerical Methods in Engineering, vol. 83, pp. 765-785, 2010.

[8] S.S. Ghorashi, N. Valizadeh, and S. Mohammadi, "Extended isogeometric analysis for simulation of stationary and propagating cracks," International Journal for Numerical Methods in Engineering, vol. 89, pp. 1069-1101, 2011.

[9] G. Haasemann, M. Kastner, S. Pruger, and V. Ulbricht, "Development of a quadratic finite element formulation based on the XFEM and NURBS," International Journal for Numerical Methods in Engineering, vol. 86, pp. 598-617, 2011.

[10] J.A. Cottrell, T.J.R Hughes, and Y. Bazilevs, Isogeometric Analysis towards Integration of CAD and FEA (first edition), A John and Wiley & Sons Ltd, Publications (UK), 2009.

[11] I. Zeid, Mastering CAD/CAM. Tata McGraw-Hill Publishing Company Ltd, 2007.

[12] N. Moes, J. Dolbow, and T. Belytschko, "A finite element method for crack growth without remeshing," International Journal for Numerical Methods in Engineering, vol. 46, pp. 131–150, 1999.

[13] T. Belytschko, and T. Black, "Elastic crack growth in finite elements with minimal remeshing," International Journal for Numerical Methods in Engineering, vol. 45, pp. 601–20, 1999.

[14] J. Dolbow, N. Moes, and T. Belytschko, "An extended finite element method for modeling crack growth with frictional contact," Computer Methods in Applied Mechanics and Engineering, vol. 190, pp. 6825–46, 2001.

[15] I.V. Singh, B.K. Mishra, S. Bhattacharya, and R.U. Patil, "The numerical simulation of fatigue crack growth using extended finite element method," International Journal of Fatigue, vol. 36, pp. 109-119, 2012.

[16] S. Shojaee, E. Izadpanah, N. Valizadeh, and J. Kiendl, "Free vibration analysis of thin plates by using a NURBS-based isogeometric approach," Finite Elements in Analysis and Design, vol. 61, pp. 23-34, 2012.
[17] H. Kapoor, and R.K. Kapania, "Geometrically nonlinear NURBS isogeometric finite element analysis of laminated composite plates," Composite Structures, vol. 94, pp. 3434-3447, 2012.